Initial Implementation of Complementary Laser Scattering Plasma Diagnostic Techniques via a Novel Transmission-Type Triple Grating Spectrograph

Kevin Finch, Songyue Shi, Jong Min Lee, Chad Pesek, Aldo Hernandez, Gerardo Gamez*
Department of Chemistry and Biochemistry, Texas Tech University

Abstract

There are many new plasma geometries and modalities being proposed to improve chemical analysis of a variety of samples. However, the underlying species behavior and mechanisms that govern such plasma-based chemical analysis are not fully understood. Therefore, it is imperative that systematic studies are carried out to monitor the fundamental parameters, including temporally-resolved maps of electron/gas temperatures and densities. The methods of choice to probe these species are laser Thompson, Rayleigh, and Raman scattering. Laser scattering diagnostic techniques have inherent spatial and temporal resolution, do not perturb the plasma (if the laser intensity is strictly controlled), and do not assume local thermodynamic equilibrium. Thomson scattering (TS) also enables the simultaneous measurement of electron temperature (T_e) and density (n_e) without the propagation of error. On the other hand, TS cross-sections are very small, and the spectral shifts are extremely close to the orders-of-magnitude higher Rayleigh signal which puts a heavy burden on maximizing transmission and contrast while minimizing the interferences from stray light. Here, the first implementation of a newly constructed transmission-type triple grating spectrograph (TGS) for plasma diagnostics of a glow discharge will be discussed. Rayleigh scattering will be used to obtain maps of gas-kinetic temperature, while allowing the absolute calibration of the electron temperature and density measurements by TS. Raman scattering will be used to provide insight into vibrational transitions when the relevant molecular species are available. The features of the TGS will allow the measurement of electron and plasma gas fundamental parameters with higher sensitivity and at positions much closer to relevant surfaces, for example, the glow discharge region close to the cathode that was not accessible in earlier studies due to stray light limitations.

Introduction

Electron interactions are the primary mechanism of kinetic energy transfer in ionized gases and spatiotemporal knowledge of these species is necessary for local optimization to occur for improved chemical analysis performance [1]. Using Thomson, Rayleigh, and Raman scattering we can gain insight into the electron interactions while also elucidating gas-kinetic maps and molecular rotational temperatures. Due to TS having an extremely small cross-sectional area and λ shifts very close to the laser λ, it is very difficult to accurately probe due to the many orders-of-magnitude higher Rayleigh signal. This requires TS instruments to have high optical throughput and stray light rejection, while maintaining the necessary contrast for spectral shifts close to the laser λ [2]. The novel TGS presented here utilizes transmission-type holographic gratings for compact instrument design and low f-number lenses for increased light collection [3]. A notch filter is created by the first two stages being set in subtractive mode with a removable physical mask in between to minimize the Rayleigh signal and stray light, while providing the high contrast of the close λ shifts [3].

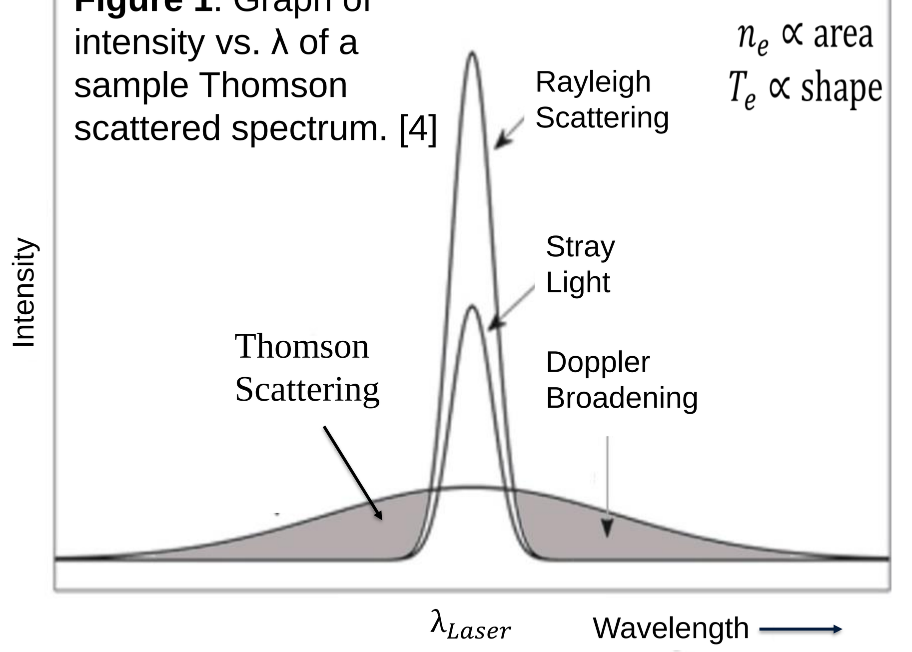

Figure 1. Graph of intensity vs. λ of a sample Thomson scattered spectrum. [4]

Triple Grating Spectrograph Schematic

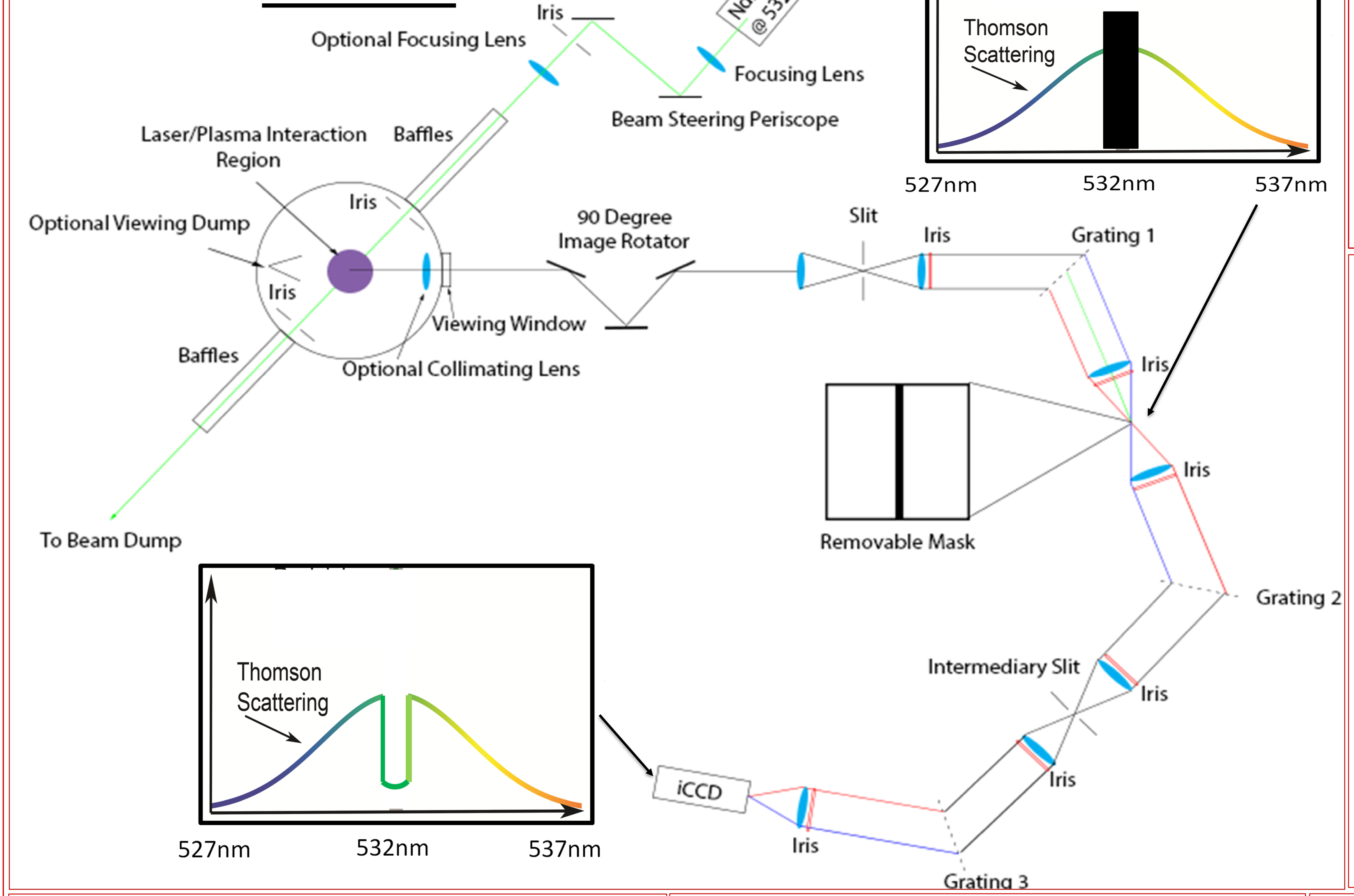

Laser/Plasma Interaction Region

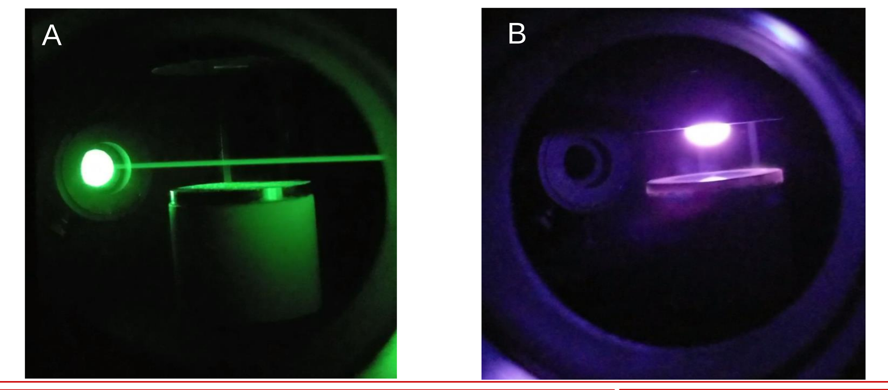

Figure 8. Image of glow discharge chamber with (A) pulsed Nd:YAG laser at 10 Hz, 108 mJ, no plasma and (B) Continuous DC plasma on at 3.21 torr Ar, 400 V, 70 mA, 30 cm cathode to anode, laser off.

Rayleigh Calibration

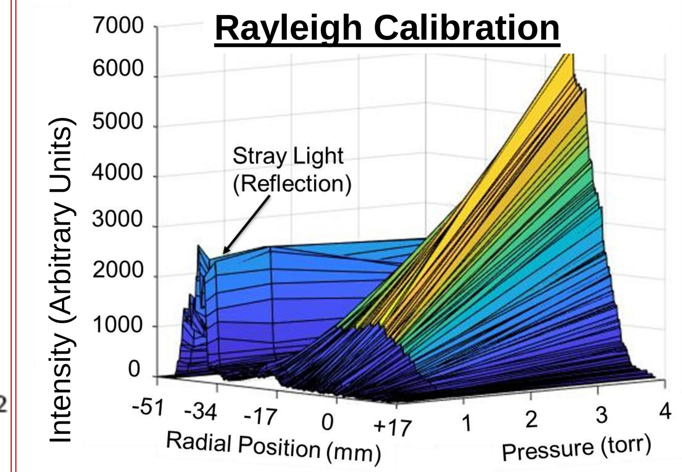

Figure 9. Rayleigh calibration of argon pressure vs. intensity with plasma off (cf. Fig. 8A), as a function of radial position. The stray light value is shown by the intensity value at 0 pressure. The difference in slopes across the region of interest is caused by the depth of focus from the collection lens used. (Compound Lens, 12x demagnification)

Gas-Kinetic Temperature Map

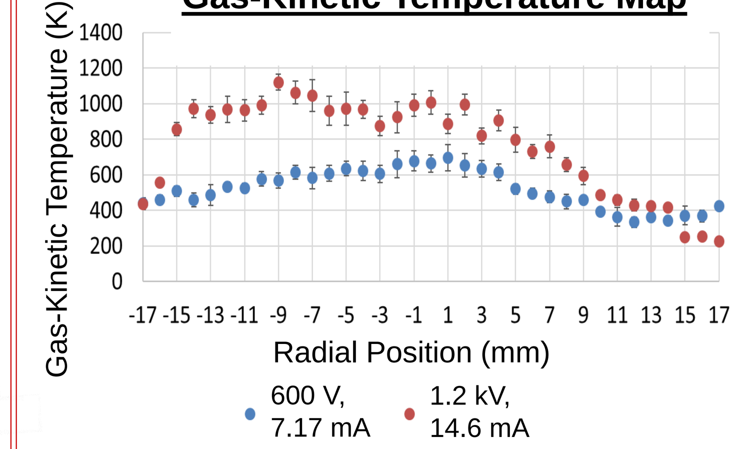

Figure 10. Gas-kinetic temperatures as a function of radial position in the plasma. Probed 18 mm from cathode via Rayleigh Scattering using two different applied powers. DC continuous plasma (cf. Fig. 8B) at 1.6 torr. Error bars show uncertainties in the slope of the linear regression (cf. Fig. 9) at each radial position. (Compound Lens, 12x demagnification)

Linearized Thomson Scattering Profile

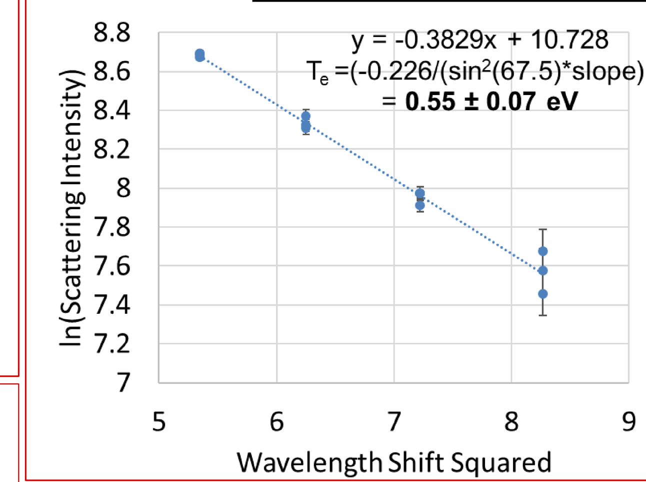

Figure 16. Linearized Thomson cross-section, using the positive wavelength shifts, at a radial position of 0 mm. The slope is proportional to the T_e which is shown. Error bars show the standard deviation of three radial positions that span a total of 0.39 mm. The error in the T_e is the uncertainties of the slope in the linear regression. 1.9 torr, -765 V, 4 mA, 0.1 slpm flow rate. (Pair of Singlets)

Study	Pressure	Current and Voltage	Distance from Cathode	Wavelength Shift (nm) Squared	(T_e)
This study	1.9 Torr	4 mA, -765 V	5 mm	5-8	0.55 ± 0.7 eV
Gamez et. al. 2004	1 Torr	5 mA, - 600 V	4 mm	3-8	~ 0.88 eV
Gamez et. al. 2004	1 Torr	5 mA, -600 V	6 mm	0-5	~ 0.28 eV

TGS Flatfield Characterization

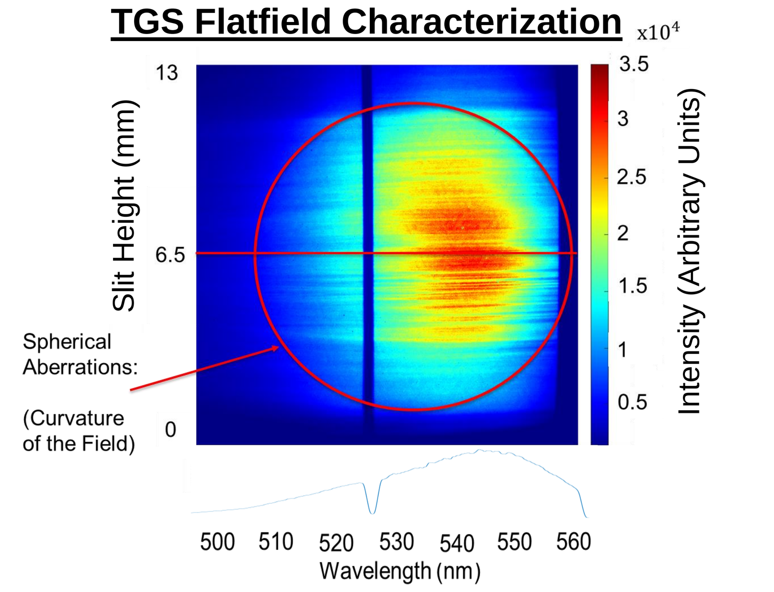

Figure 2. Flatfield image (LED Lamp at Slit) shown after background subtraction and 50 frame average. The dark vertical section shows the location of the mask. Aberrations in the spatial and spectral dimensions are evident. Red line shows the radial location of the cross-section intensity profile at the bottom.

TGS Spectral Calibration

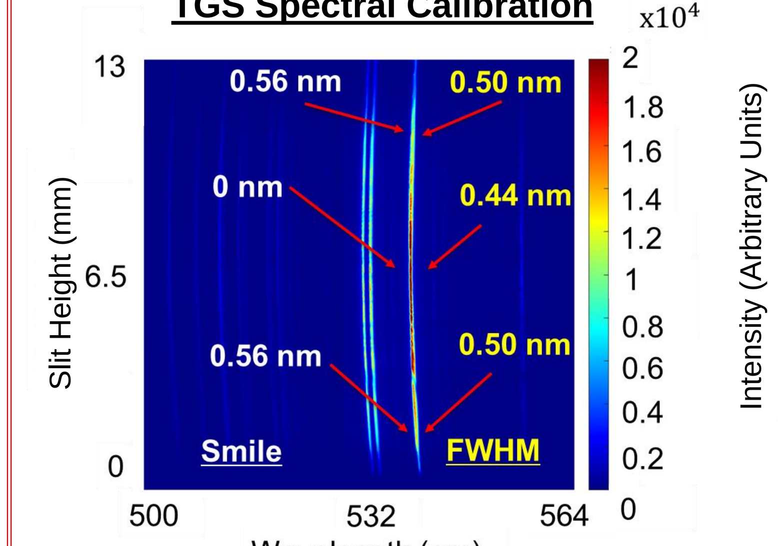

Figure 3. Spectral resolution image (Neon Pen Lamp at Slit) shown after background subtraction and 50 frame average. The "smile" (curvature of slit image) is evident across the detector. The spectral resolution is represented by the full width at half maximum (FWHM) is shown above and was calculated using the 540 nm line.

Rotational Raman Scattering

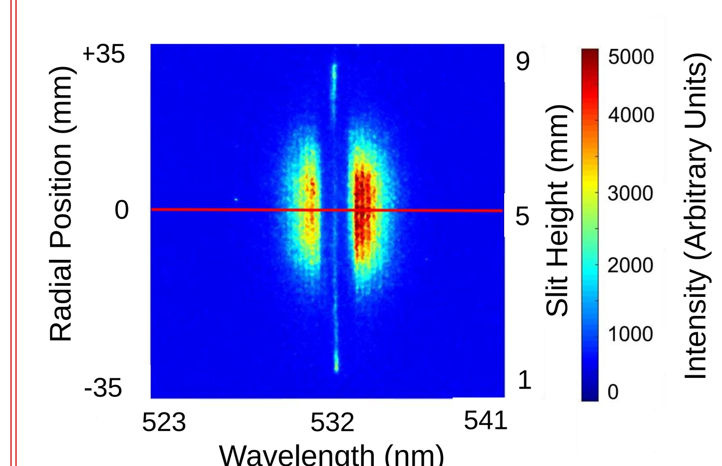

Figure 11. Rotational Raman spectrum after 3x3 median filter, of nitrogen at atmospheric pressure (cf. Fig 8A). Contrast at top and bottom of field deteriorates due to spectral smile. Red line shows the radial position of the cross-section in Fig. 12. (Compound Lens, 12x demagnification)

Raman Scattering Profile

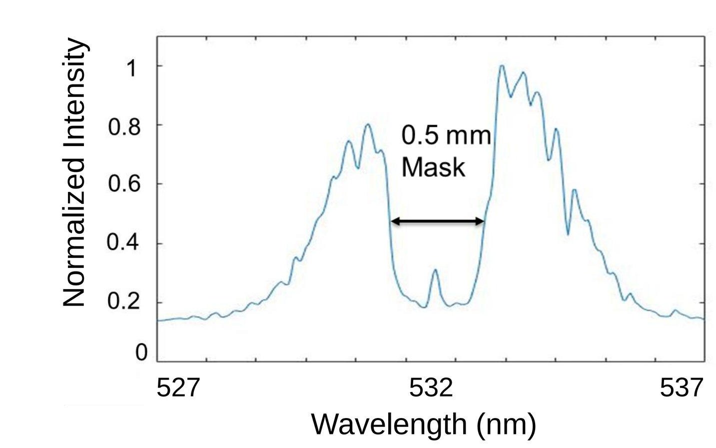

Figure 12. Rotational Raman cross-section taken at a radial position of 0 mm. The mask used is 0.5 mm wide. Rotational transitions are evident on both sides of the mask, higher at longer wavelengths due to Stokes. (Compound Lens, 12x demagnification)

TGS Spatial Characterization

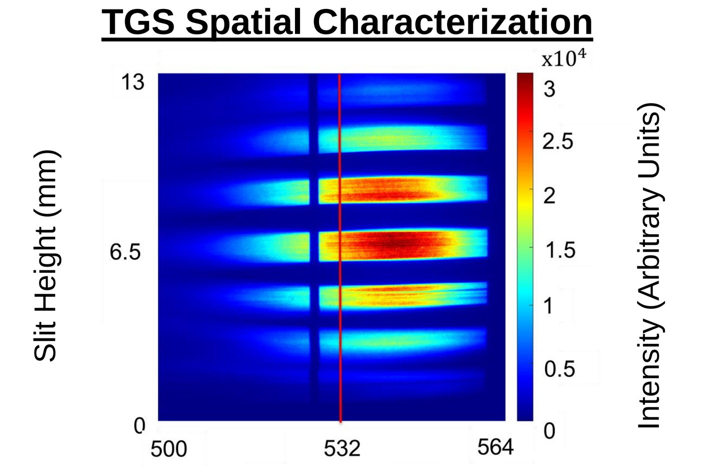

Figure 4. Spatial resolution image (LED Lamp at Slit) shown after background subtraction. Edge to edge mask lines are approximately 1 mm in diameter. Red line shows the wavelength of the cross-section in Fig. 5.

Edge Function: FWHM of 1st Derivative (mm)

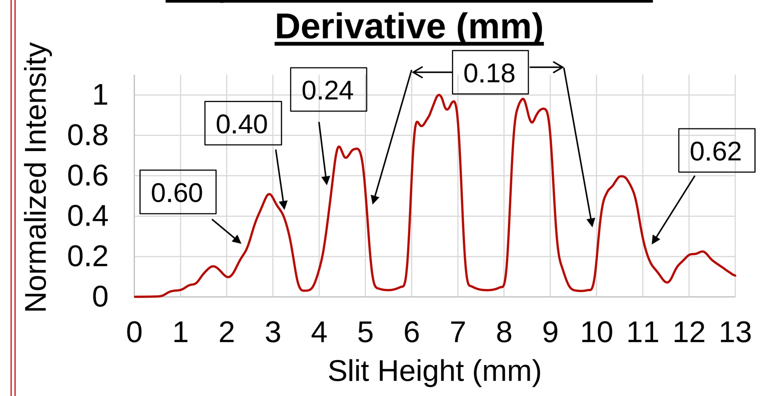

Figure 5. Spatial resolution cross-section shown at 532 nm. A 3rd order, 21-pixel window Savitzky-Golay filter and 11 pixel moving average were applied. The edge function values range from 0.60 mm to 0.18 mm.

Rotational Raman Scattering

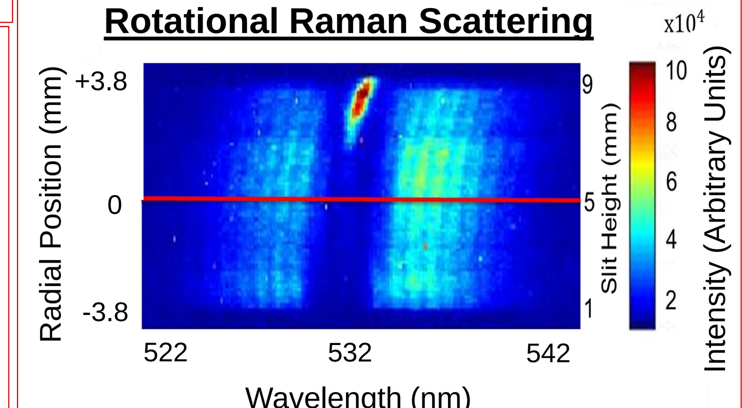

Figure 13. Rotational Raman spectrum after 3x3 median filter, of nitrogen (cf. Fig. 8A) at atmospheric pressure. Mask is 0.33 mm wide. Red line shows the radial position of the cross-section in Fig. 14. About 100x signal gain achieved! (Pair of Singlets, 1 to 1 demagnification)

Raman Scattering Profile

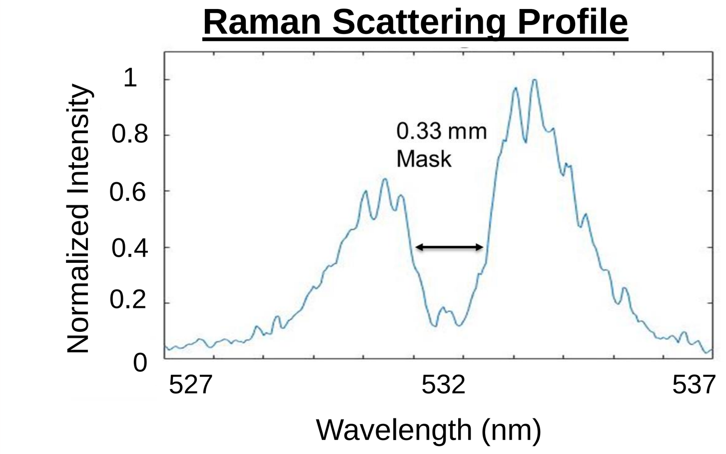

Figure 14. Rotational Raman cross-section taken at a radial position of 0 mm. The mask used is 0.33 mm wide. Rotational transitions are evident on both sides of the mask, higher at longer wavelengths due to Stokes. (Pair of Singlets, 1 to 1 demagnification)

TGS Mask Efficiency

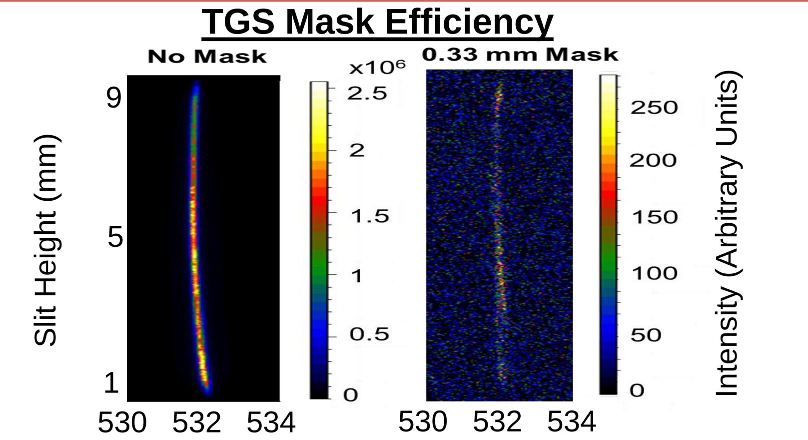

Figure 6. Laser line (532.06 nm) images shown after background subtraction, taken at slit. (A) Image taken without the mask and (B) with 0.33 mm wide mask aligned at 532 nm. Both images were taken under the same iCCD conditions.

TGS Contrast

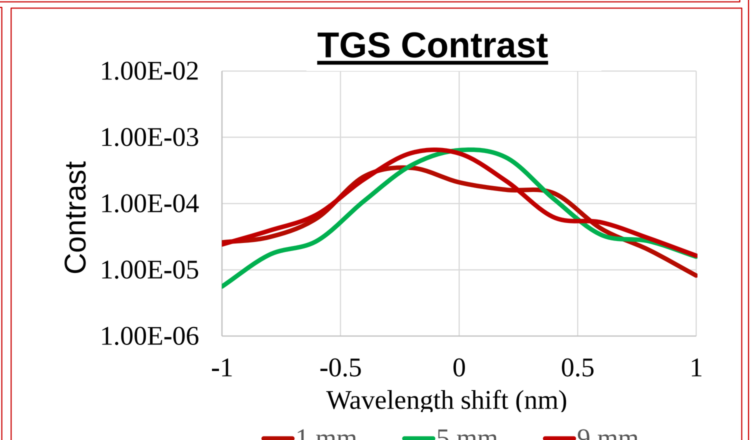

Figure 7. Contrast shown at three different spatial locations (1, 5, and 9 mm, cf. Fig. 6) using 0.33 mm wide mask after 3x3 median filter and 5-sigma Gaussian filter.

Thomson Scattering

Thomson Scattering Intensity Profile

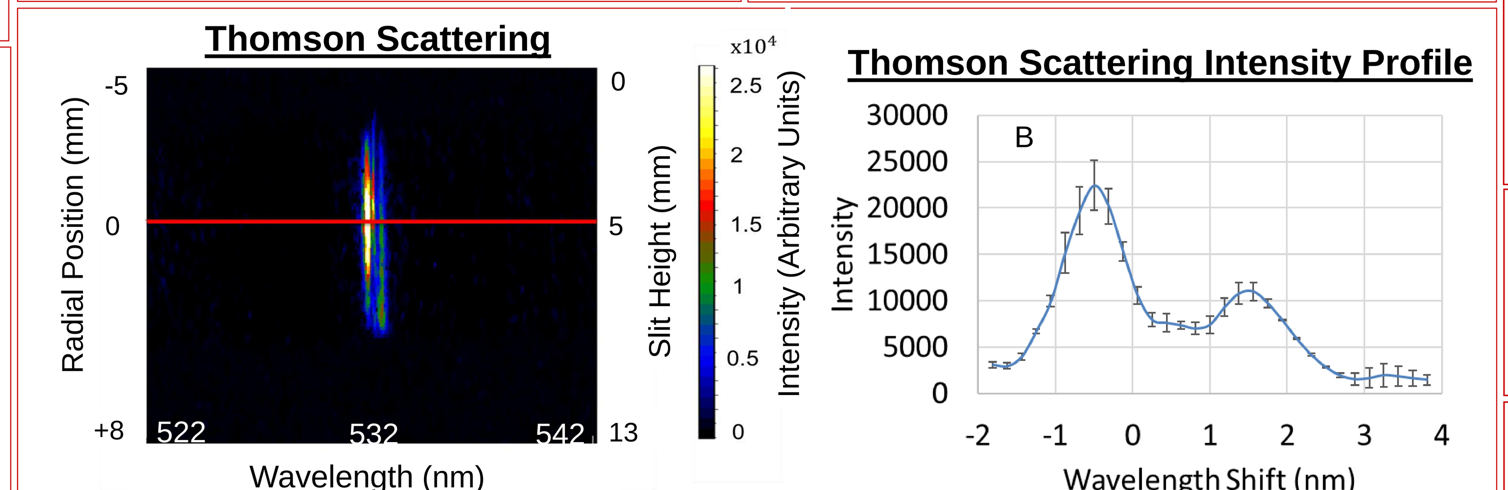

Figure 15. (A) Thomson scattering spectrum taken at a gas pressure of 1.90 torr with the plasma on (cf. Fig. 8B, -765 V, 4 mA). Doppler shifted scattering is seen on both sides of mask. Due to spectral smile there are higher intensities at shorter wavelengths. Red line shows the radial position of the intensity profile shown in (B). (Pair of Singlets, 1 to 1 demagnification)

Triple Grating Spectrograph Specifications

Laser	Nd:YAG @ 532 nm
Laser Focusing Lens	50 mm Ø f/21 biconvex
Image Rotator	K-mirror design
Collection Lens(es)	50 mm Ø f/1.2 Compound or 50 mm Ø f/2 planoconvex singlet x2
TGS Lenses	50 mm Ø f/2 aspheric x6
Gratings	50.8 mm Ø, 1800 lines/mm, 28.6° AOI @ 532 nm
Slits	13 mm height x 52 µm width
Removable Mask	13 mm height x 0.33 mm width
Irises	39.5 mm x 45 mm elliptical
iCCD Camera	13.3 mm x 13.3 mm detector size, 13 µm pixel width
Optional Viewing Dump	Offset welders glass placed at 15° angle

Conclusion

Thomson (Fig. 15), Raman (Fig. 11, 13), and Rayleigh (Fig. 9) scattering measurements were successfully achieved using the novel TGS. Gas-kinetic temperatures (Fig. 10) and electron temperature (Fig. 16) were successfully measured from a DC GD under OES conditions and are comparable to previous studies under similar conditions [5]. A "jitter" in the trigger timing of the laser prevented narrow gate widths (< 250 ns) to be realized and resulted in an increase in the plasma background of about 100x, thus limiting sensitivity.

Future Work

Image processing corrections will be applied to the flatfield image (Fig. 2) to remove the spectral shape and the "smile" for use in correcting images for system aberrations. An improved contrast characterization will be performed using neutral density filters to increase the dynamic range of the measurement. An absolute Rayleigh scattering calibration with the pair of singlets collection optics will be taken, to allow for electron density determination. Rotational temperatures of nitrogen will be obtained from Raman scattering through simulated spectra. Laser scattering diagnostics will be implemented for GD under elemental mapping conditions (10-30 torr, kHz pulsed power).

Acknowledgments

Dr. Gerardo Gamez Research Group
TTU Machine Shop: Scott H. & Jamar M.
TTU Electrical Shop: Vince W.
National Science Foundation under CHE - 1610849
J.T. and Margaret Talkington Fellowship
Phi Kappa Phi: Love of Learning Award
Indiana University: Prof. G. M. Hieftje Laboratory
Ming Sun Family Graduate Research Scholarship
Ginny Shen Lin Scholarship

References

[1] Gamez G., et al. (2003) J. Anal. At. Spectrom., 18, 680-684
[2] A F H van Gessel, et. Al., (2012) Plasma Sources Sci. Technol. 21 015003
[3] Finch K., et al. (2020) J. Anal. At. Spectrom., Advance Article, DOI: 10.1039/D0JA00193G
[4] Yong W., et al., (2017) Plasma Sci. Technol., 19, Num. 11, 5403
[5] Gamez G., et al., (2004) Spectrochimica Acta Part B., 59 (4), 435-447.